Photoinduced charge transfer from quantum dots measured by cyclic voltammetry

Micaela K. Homer, Ding-Yuan Kuo, Florence Y. Dou and Brandi M. Cossairt*

Department of Chemistry, University of Washington, Box 351700, Seattle, WA 98195-1700.

*cossairt@uw.edu

Abstract

Measuring and modulating charge-transfer processes at quantum dot interfaces are crucial steps in developing quantum dots as photocatalysts. In this work, cyclic voltammetry under illumination is demonstrated to measure the rate of photoinduced charge transfer from CdS quantum dots by directly probing the changing oxidation states of a library of molecular charge acceptors. The voltammetry data demonstrates the presence of long-lived electron donor states generated by native photodoping of the quantum dots as well as a positive correlation between driving force and rate of charge transfer. Changes to the voltammograms under illumination follow mechanistic predictions from classic zone diagrams and electrochemical modeling allows for measurement of the rate of productive electron transfer. Rate constants for photoinduced charge transfer on the order of 10^4 $M^{-1}s^{-1}$ are calculated, which are distinct from the picosecond dynamics measured by conventional transient optical spectroscopy methods and are more closely connected to the quantum yield of light mediated chemical transformations.

TOC Graphic

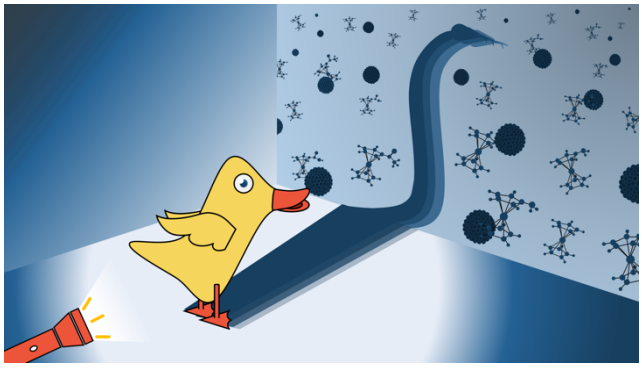

Introduction

Photoinduced charge separation is a key process in photosynthesis, and artificial photocatalytic systems rely on the same process for chemical storage of solar energy.[1] Quantum dots (QDs) have long been promoted as ideal photosensitizers for photocatalysis and photovoltaic applications due to their high extinction coefficients, electronic tunability, and solution processability,[2] but efficient extraction of high energy charge carriers from QDs remains a design challenge.[3] Photoinduced charge transfer from QD donors requires transfer of charges across the interface between the inorganic QD core and a molecular cocatalyst or substrate in solution.[4,5] Photoinduced charge transfer from QDs is complicated by the high prevalence of defect electronic states in the QD[6,7] and the covalent and non-covalent interactions between

the QD, the insulating ligand shell, and the charge acceptor.[8] Conventional models of charge transfer in molecular systems (e.g. the two state system described by the Marcus formalism) are therefore insufficient to predict the rate of useful charge extraction from QDs, prompting experimental exploration.[9]

Photoluminescence spectroscopy[10–12] and transient absorbance spectroscopy[13,14] are frequently employed to determine rates of photoinduced charge transfer in QD systems. In these experiments, the charge transfer process measured is pseudo-unimolecular with a first-order rate constant. This rate presumes pre-adsorption of the charge acceptor to the QD and does not consider freely diffusing charge acceptors nor the dynamic noncovalent chemical interactions between the QD and acceptor.[10,13,15,16] While determination of the first order rate has utility, especially when compared with other unimolecular photophysical processes such as electron/hole recombination, there is a large disconnect in the literature between the time scale for this fundamental process (picoseconds) and the time scale of photocatalytic reactions (minutes)[17,18]. It may then be counterintuitive that several reports have found that the rate-limiting step of photocatalysis is charge transfer from nanocrystal photosensitizers to substrate or cocatalyst.[18–21] This disconnect begs us to consider that the spectroscopic first order rate of charge transfer does not accurately report on the rate of production of charge separated states, and instead a new method is needed to understand processes taking place on the same time scales as chemical reactions.[3]

Alternatively, charge transfer can be rationalized as a bimolecular reaction that is first order with respect to both the charge donor (catalyst) and acceptor (substrate).[22] Then the rate of photoinduced charge transfer in QD systems may be framed as first order with respect to both the excited QD and the charge acceptor. The two species must first collide before charge can be extracted from the QD, and the rate of observed charge extraction will depend on the frequency of collisions, the rate of the fundamental photophysical process observed by time-resolved spectroscopies, and the fraction of collisions that allow strong electronic coupling between the QD and charge acceptor.

We turned to cyclic voltammetry (CV), a measurement tool that directly probes the changing oxidation state of a redox active small molecule. CV has been employed in homogeneous electrocatalysis literature as a probe for the changing oxidation states of a molecular electrocatalyst,[23] and has been theorized to be a tool for evaluating molecular photoelectrocatalysis.[24] We hypothesized that CV could be extended to systems involving photoinduced charge transfer from QDs. In the electrocatalysis literature, one of the simplest and most well-understood systems is described by two reactions: the oxidation and reduction of the electrocatalyst at the electrode, and the catalytic reaction in which the electrocatalyst transfers charge to substrate. This mechanism is termed E_rC_i'. In such a system, the CV is modulated as compared to CVs in the absence of substrate, and this modulation can be quantified to obtain the rate constant for the catalytic reaction. For a thorough review of this technique, see Rountree *et al.*[23] In this work we aim to analogously measure the rate of productive charge extraction from QDs using CV (**Scheme 1**). We believe that the rates obtained through this measurement (k_{PCT}) will accurately reflect the extraction of charge from QDs and will bridge the gap in time scales between photophysics and chemical transformations.

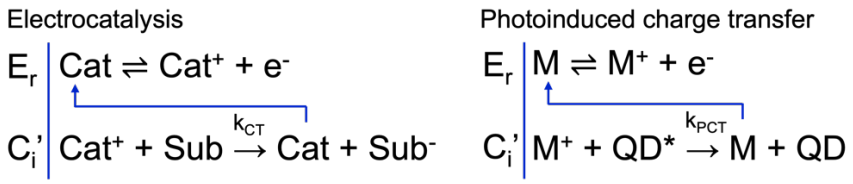

Scheme 1. The E_rC_i' mechanism employed in the electrocatalysis literature (left), and the extension of this mechanism to photoinduced charge transfer from an excited QD (QD*) to a molecular acceptor (M). In this work, k_{PCT} represents the rate constant of photoinduced charge transfer.

Photoelectrochemistry cell design

A traditional three-electrode electrochemical cell was modified for *in situ* illumination. A 448 nm LED (Luxeon Star, equipped with a 12° beam optic, FWHM 20nm) was positioned under a quartz cuvette with a polished bottom and open top (**Figure 1**). The cuvette was placed on top of the LED. The LED was powered by a DC power supply (Nice-Power). The driving current was 0.2-0.8A, corresponding to approximately 0.3-1.1W of illumination.

Holes were drilled in a cuvette cap for the three electrodes and the glassy carbon disc working electrode (BASi) was epoxied to the cap, ensuring the light had a constant and known pathlength (0.67 mm) through the solution to the active area of the working electrode. The pathlength is small to minimize undesired convection effects on the voltammogram from photoirradiation,[25] as well as to decrease the amount of light that is attenuated by the highly absorbent QDs in solution before reaching species near the working electrode surface. The counter electrode was a platinum wire, and the pseudo-reference electrode was a silver wire in a ceramic-fritted glass tube (Pine) filled with 0.1M [TBA][$B(C_6F_5)_4$].

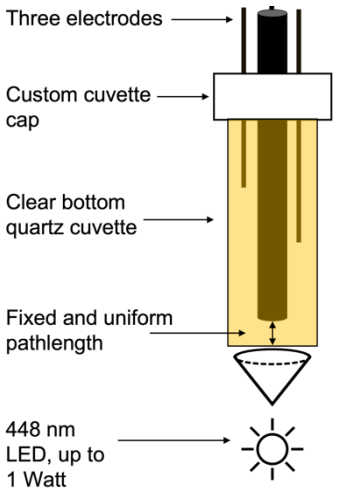

Figure 1. Drawing of the electrochemical cell for voltammetry under illumination.

Solvent and electrolyte design for photoelectrochemistry

The selection of solvent and supporting electrolyte is critical to obtaining electrochemical measurements suitable for quantitatively monitoring photoinduced charge transfer. The solvent is being used as a charge

transfer mediator, both from the working electrode to the redox probe and between the QD and the redox probe, so it must be polar to minimize internal resistance. The solvent must also allow high electrolyte concentration and have a wide electrochemical window to screen a wide range of redox probes. These electrochemical considerations are general, but for photoelectrochemistry, the solvent must additionally not undergo any photodecomposition nor reactivity with excited QDs. Previously, our group found a mixture of 9:1 THF:MeCN was able to suspend oleic acid capped QDs with low internal resistance.[26] However, when THF was used in this work, the CV exhibited current crossover (**Figure S1**), an unusual observation that indicates the product of Faradaic oxidation on the forward scan of the CV is chemically converted to another species that is more easily oxidized and observed on the backward segment.[27] Given prior observation that THF degrades under illumination to form reactive radicals,[28] THF is not a suitable solvent for this study.

Dichloromethane was another attractive solvent due to its modest polarity and ability to disperse as-synthesized QDs. Unfortunately, CVs under illumination displayed oscillations in the current, especially in the diffusion limited regime (**Figure S2**). These oscillations were the result of gas bubbles evolving and reaching the surface of the working electrode, which was observed visually during illumination of the sample. Headspace analysis detected production of methane after illumination (**Figure S3**). With these observations, as well as prior observation of dehalogenation of CH_2Cl_2 with QD photocatalysts[29], we conclude that the system photocatalytically dehalogenates CH_2Cl_2 to methane, so CH_2Cl_2 is not a suitable choice for photoelectrochemical measurement.

Another limitation in solvent choice is the solubility of the QDs, as QDs are often natively capped with aliphatic ligands that prevent dispersion in polar solvent at high electrolyte concentration. Ligand exchange was performed on QDs to replace the native oleic acid ligand shell with 2-[2-(2-Methoxyethoxy)ethoxy]acetic acid (MEEAA), which is known to be an amphiphilic ligand that has dissolved nanocrystals in solvents ranging from toluene to water.[3031] In our hands, 5.5 nm CdS QDs capped with this ligand are readily soluble in a variety of polar solvents, including water, acetone, and ethanol, but cannot be dispersed in some polar, aprotic solvents suitable for electrochemistry such as acetonitrile and propylene carbonate. Ultimately, benzonitrile (PhCN) was selected for this study because of the good colloidal stability of QDs in electrolyte solutions prepared using this solvent. MEEAA capped QDs in benzonitrile solution remain suspended for at least several months even in the presence of electrolyte.

Finally, the solvent and electrolyte should allow reversible CVs for all the redox probes in the absence of QDs and illumination. Using the more common tetrabutylammonium salt of the $[PF_6]^-$ anion prevented reversible redox behavior of ferrocenecarboxylic acid (FcCOOH), presumably due to the high electrophilicity of the $[FcCOOH]^+$ cation. Instead, the tetrabutylammonium salt of the weakly coordinating anion $[B(C_6F_5)_4]^-$ was used. This completely fluorinated phenyl borate is known to stabilize organometallic cations, such that the only allowed processes in the CVs were oxidation and reduction of the metal center.[32] When this anion was used in the supporting electrolyte, FcCOOH displayed nearly ideal electrochemical reversibility.[33]

Photodoping and slow electron trapping observed by CV

Upon successive scans after illumination, the CV of ferrocene, a representative redox probe, continues to distort as compared to the dark trace (**Figure 2b**). The CVs move to the right across the E_rC_i' zone diagram, from zone D to zone KD to zone KS, which by analogy to electrocatalysis literature[23] demonstrates an increase in the concentration of QDs in a charge donor state (herein represented as

[QD*]) (**Figure 2a,b**). This distortion occurs over ca. 20 minutes of illumination and then stabilizes, corresponding to a stabilization of [QD*]. This extremely long time scale until equilibration of [QD*] as compared to the speed of photoexcitation (femtoseconds) suggests that the charge donor state is not simply an exciton, but rather the product of a slow chemical process following excitation.

Previous studies have reported native n-type photodoping in cadmium chalcogenide QDs over the same timescale observed in this study, wherein after excitation a valence band hole is extracted without any added reductant, leaving behind a long-lived conduction band electron.[34,35] We expect that this n-doped QD acts as the charge donor observed in CV. To further investigate the nature of the charge donor state, we monitored the solution with successive CV scans after illumination was stopped. Over the course of ca. 20 minutes, the CV recovers back to its original dark trace as QD* is slowly depleted, thus tracking to the left along the E_rC_i' zone diagram (**Figure 2c**). Others have also reported that negatively photodoped QDs live for many minutes due to extremely slow electron trapping.[34–36] While the precise mechanism of native photodoping and subsequent charge trapping is still under investigation, this phenomenon can be observed in CV in addition to optical measurements.

After many minutes of photodoping [QD*] stabilizes, but here as in prior literature reports this concentration was not equivalent to the analytical QD concentration.[34] While [QD*] stabilizes for a given light intensity, the stable CVs of a representative redox probe, FcCOOH are not the same when the light intensity is varied. As the power is increased from 0.33 W to 1.14 W, the stable CV is distorted further from the dark CV, again well matched to traversing to the right across the zone diagram (**Figure 2d**). This observation indicates that although at any given light intensity [QD*] reaches an equilibrium, not all QDs are photodoped. It is expected that as light intensity is further increased, the CV would eventually stop distorting once the maximum concentration of n-doped particles is reached, but this light-saturated regime is not observed due to the limited power output of the LED light source.

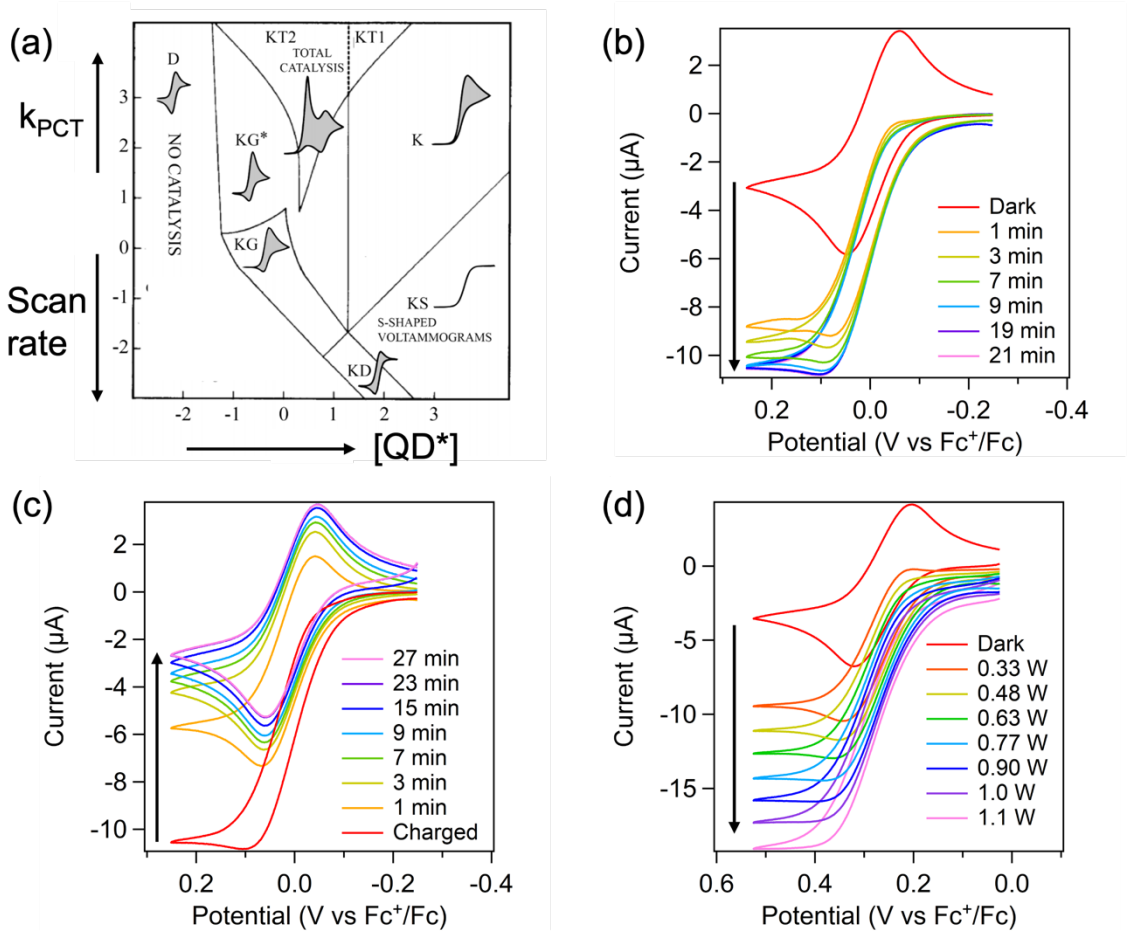

Figure 2. (a) The zone diagram for the E_rC_i' mechanism, adapted from Rountree et al.[23] (b) Photodoping monitored by successive CV scans of Fc after illumination begins. (c) Depletion of charge donor states by slow electron trapping monitored by CVs of Fc after illumination ends. (d) Light intensity dependence on equilibrated CVs of FcCOOH. 0.1M [TBA][$B(C_6F_5)_4$], benzonitrile, glassy carbon working, Pt counter, Ag wire pseudo reference electrodes, 10 mV/s.

Electron acceptors: Co(Cp)(dppe), $FcNH_2$, Fc, FcCOOH, $FcCOCH_3$

When QDs are added to solutions of Co(Cp)(dppe) (Cp = cyclopentadienyl, dppe = 1,2-Bis(diphenylphosphino)ethane), aminoferrocene ($FcNH_2$), ferrocene (Fc), FcCOOH, or acetylferrocene ($FcCOCH_3$) the CV remains unchanged for traces without illumination. This observation, alongside no observed change in the dark open circuit potential, demonstrates that none of these probes exhibit charge transfer reactions with the QDs in the dark. Furthermore, the magnitude of the current does not change upon addition of QDs, indicating no adsorption to the QDs. If indeed there was adsorption, the effective diffusion coefficient of the redox probes would decrease due to the much larger QD, decreasing the current measured in CV. Previously, FcCOOH was observed to bind to oleate-capped CdSe QDs using CV through carboxylate-carboxylate exchange with the native ligand shell.[26] In contrast, FcCOOH does not undergo similar exchange with MEEAA-capped CdS QDs. The lack of exchange is rationalized by the lower pKa of MEEAA (pKa = 4.43)[37] compared to oleic acid (pKa= 9.85)[38].

The CVs of solutions containing Co(Cp)(dppe), $FcNH_2$, Fc, FcCOOH, and $FcCOCH_3$ and QDs all distort under illumination, and stabilize after several minutes as described in the photodoping discussion above. For all probes at all light intensities and scan rates, there is an increase in oxidative current and decrease of reductive current as compared to dark traces (**Figure 3a**). This implies that under illumination, the oxidized probe, M^+, is reduced to M through photoinduced electron transfer from the quantum dot. To elaborate, during the oxidative segment of the CV, as the potential is increased, M is oxidized to M^+ at the working electrode (E_r in **Scheme 1**). Then, some of this M^+ is reduced back to M by a photodoped QD* (C_i in **Scheme 1**). This additional M can be oxidized at the electrode and so on, increasing the measured oxidative current as compared to the dark scan. On the reductive segment, M^+ formed at the electrode has been depleted by photoinduced charge transfer, so the magnitude of the reductive current is decreased. At steady state, the rate of M^+ depletion is equal to M^+ generation at the working electrode. $[M^+]$ is zero at the electrode surface, so there is no reductive current.

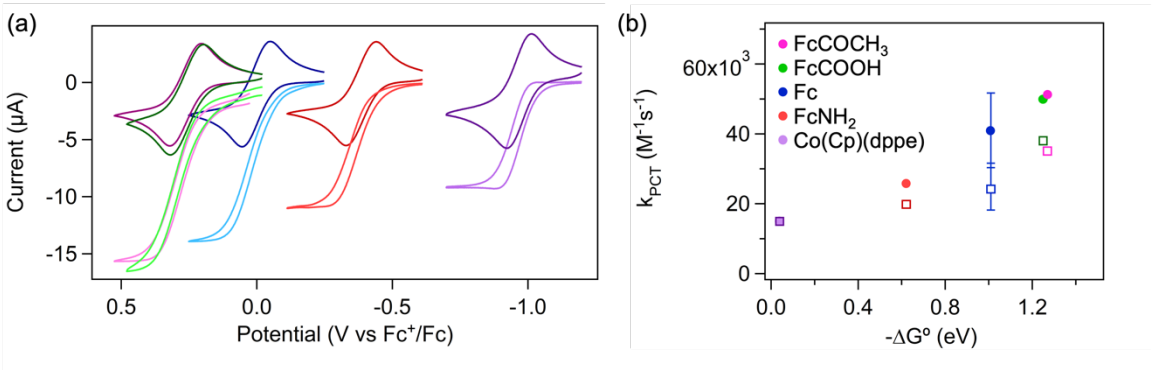

Figure 3. (a) CVs of the series of electron acceptors without illumination (dark colors) and with 1.1 W illumination (light colors). From left to right, the redox probes are $FcCOCH_3$ (fuchsia), FcCOOH (green), Fc (blue), $FcNH_2$ (red), and Co(Cp)(dppe) (purple). (b) The rate constant for photoinduced charge transfer under 0.77 W illumination determined mathematically (open squares) and by electrochemical modeling (closed circles), plotted against the estimated driving force for electron transfer (SI for details). Error bars on the Fc data point were obtained from quadruplicate experiments.

Mathematical Determination of E_rC_i' Rate Constant for Co(Cp)(dppe), $FcNH_2$, Fc, FcCOOH, $FcCOCH_3$

The rate constant for the photoinduced charge transfer reaction (C_i' in the E_rC_i' mechanism) can be determined mathematically from voltammograms when in zone KD or KS, which are the zones observed in this work. In these experiments, the observed rate in the experiment (k_{obs}) is related to the scan-rate independent plateau current (i_c) observed in zone KS and zone KD by Equation 1, where n is the number of electrons transferred at the electrode, and i_p and v are the peak current and scan rate for a reversible, dark experiment. Notably, this equation does not require any knowledge of the diffusion coefficient or concentration of the redox probe because the currents are taken as a ratio.

$$\frac{i_c}{i_p} = \frac{1}{0.446}\sqrt{\frac{RT}{nF\nu}k_{obs}} \quad \text{(Eq. 1)}$$

A plot of i_c/i_p against the inverse square root of scan rate for several dark scans yielded a straight line with a slope related to k_{obs} and constants only **(Figure S4)**. The intrinsic rate constant, k_{PCT}, was related to k_{obs}

by Equation 2, where [QD*] is the concentration of n-doped QDs and is assumed to be constant during the experiment.

$$k_{obs} = k_{PCT}[QD^*] \quad \text{(Eq. 2)}$$

As described in the photodoping section, a light-saturated regime was never obtained for these materials, so not all QDs are n-doped. We assume for these calculations that [QD*] is equal to the analytical concentration of QDs, which is a reasonable estimate considering others have estimated in similar systems the majority of particles are n-doped.[34] Regardless of the precise value of [QD*], it should be the same for all experiments irrespective of the redox probe, so the relative rate constants are correct, as are the order of magnitude of these rate constants. The forward rate constant, k_{PCT}, is a direct reporter on the rate of effective charge extraction and is distinct from values obtained spectroscopically and is plotted against the estimated driving force for electron transfer, which was calculated by the difference between estimating the band edge potentials and probe redox potential **(Figure 3b).** See SI for calculations of driving force.

Electrochemical Modeling for Co(Cp)(dppe), $FcNH_2$, Fc, FcCOOH, $FcCOCH_3$

In this set of experimental conditions, only zones D, KD, and KS were observed, but in other systems reaching these zones may be experimentally constrained, precluding the use of the direct mathematical determination of the rate constants as described above. To generalize our method, we turned to electrochemical modeling of CVs in DigiElch, which has been previously used by our group to determine the thermodynamic and kinetic parameters associated with exchange of native oleic acid ligands for ferrocene and ferrocenium derivatives.[26] This powerful technique allows the fitting of many parameters relevant to the electrochemical experiment, so care must be taken to avoid overfitting the system. With each additional reaction added to the model there are more unknown variables to be fit, so we only allow three reactions in the model. These processes are the two reactions in the E_rC_i' reaction mechanism with a third reaction added to account for regeneration of the donor state *via* illumination. While these three reactions are a simplification of the many photophysical and chemical processes in the system, this generalization allows us to probe the effective rate of charge extraction.

We determined some parameters independently of photoelectrochemical experiments to minimize the number of values that are allowed to float during the general fitting. The reduction potential (E^0) and the heterogeneous electron transfer rate constant (k_s), and either concentration or diffusion coefficient for each probe are first obtained by fitting CVs without illumination. These values are assumed to be unchanged during experiments under illumination. The analytical concentration of M must be known to obtain the other parameters to be fit but can be complicated because of the sublimation of some metallocenes during sample preparation. For Fc, we assume that the analytical concentration is exactly the targeted concentration (4 μmol in 2.8 mL). Then, the diffusion coefficient of Fc, E^0 and k_s, are fit to the data for a series of CVs with varying scan rate. We then assume that the substituted ferrocenes have approximately the same diffusion coefficient as Fc ($4.67*10^{-6}$ cm^2/s). Then, we determine the analytical concentration, along with E^0 and k_s by fitting the dark scans for $FcNH_2$, FcCOOH, and $FcCOCH_3$. For Co(Cp)(dppe), we assumed that the concentration was equal to the targeted concentration and fit the data to determine E^0, k_s, and the diffusion coefficient.

Because the photoinduced charge transfer reaction depletes QD* at the electrode, a third reaction to regenerate QD* after electron transfer must be included in the model. To maintain thermodynamic

consistency, the regeneration of QD* requires the photon to be explicitly written as a reagent, or "hν" in the electrochemical model. The diffusion coefficient of hν and the concentration of hν are set to extreme values to artificially force the photocharging step to be fast compared to photoinduced charge transfer and to force [QD*] to be equal to the analytical concentration of the QDs. The diffusion coefficient of hν is set to three orders of magnitude larger than that of M (0.01 cm^2/s), the concentration is set to five orders of magnitude larger than [QD] (0.75M). Then, when the data set for Fc is modeled, the forward rate constant and equilibrium constant for the photocharging step are allowed to float. These values do not have any physical meaning, because buried in them are the assumptions for parameters of hν. Once the rate and equilibrium constants for photocharging are fit for the Fc data, they are assumed to be equal for all experiments with the same [QD] and the same light intensity.

By forcing the photocharging reaction to be fast and using the dark traces to model E_r, only the photoinduced charge transfer reaction of interest remains to be fit. No simulation runs converged well for the value of the equilibrium constant for the photoinduced charge transfer reaction. This observation makes reasonable chemical sense, as the reaction is expected to be irreversible. The backward reaction would require injecting an electron from M to QD, which was not observed *via* open circuit potential measurement when QD and M are combined. With so much uncertainty in the very slow rate of the backward reaction, this equilibrium constant was set to a very large value (10^9), forcing the backward rate to be small and not influential in the model. In sum, if the backward charge transfer reaction is forced to be slow and repopulation of the donor state (3) is forced to be fast, then the forward photoinduced charge transfer reaction is the rate limiting chemical reaction in the model and k_{PCT} is fit.

Using this modeling procedure described above, we fit a series of CVs with varying scan rate. The resulting simulated CVs are well matched to the experimental data that show progression from zone KS to KD to D as the scan rate is increased (**Figure 4**), adding credibility to the simplifications made in the mechanism. The full series of electron acceptor probes were modeled, and values of k_{PCT} are plotted in **Figure 3**.

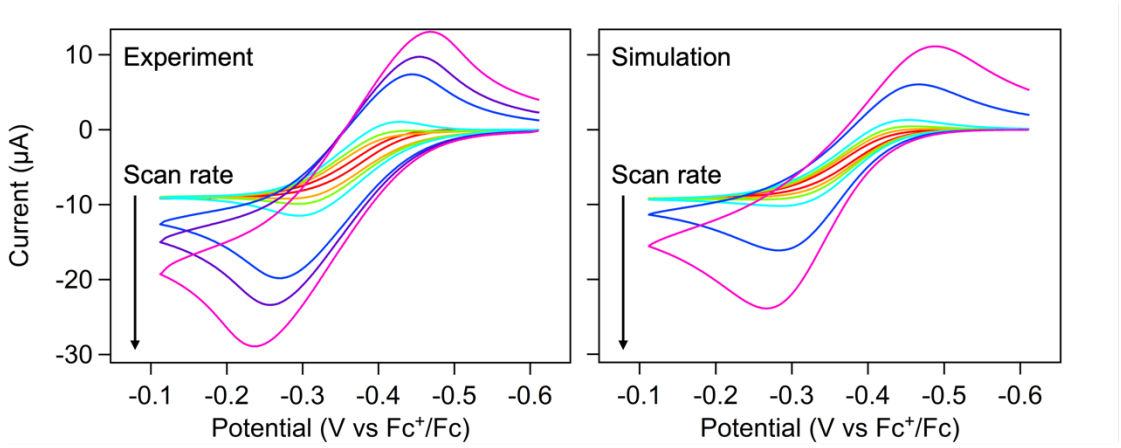

Figure 4. Comparison of the experimental data (left) to the simulated data (right) with varying scan rate. 0.1M [TBA][$B(C_6F_5)_4$], benzonitrile, glassy carbon working, Pt counter, Ag wire pseudo reference electrodes, scan rate was varied from 5 mV/s (red) to 250 mV/s (fuchsia).

Results and Discussion of Photoinduced Charge Transfer to Co(Cp)(dppe), $FcNH_2$, Fc, FcCOOH, $FcCOCH_3$

Using both mathematical determination of charge transfer as well as electrochemical modeling, k_{PCT} was determined for the range of electron accepting probes. When comparing the mathematical determination and the modeling results (**Figure 3**), k_{PCT} was generally lower using the mathematical method, though still of the same order of magnitude and displaying the same trends. Unsurprisingly, with larger driving force, k_{PCT} monotonically increases in both methods of determination. This observation is well supported by existing QD literature, wherein the Marcus inverted region is never observed and photoinduced charge transfer from quantum dots is better explained by an Auger-assisted photoinduced charge transfer model.[9,39] While others have demonstrated a similar relationship between driving force and rate of charge transfer, [9,11,40,41] we were uniquely able to measure this through CV.

We have demonstrated that the driving force for photoinduced charge transfer is the critical factor controlling k_{PCT} rather than chemical identity. FcCOOH and $FcCOCH_3$ have nearly the same E^0 but have different chemical interactions with solvent, electrolyte, and the QD ligand shell. Despite these differences, the k_{PCT} values for these two redox probes are nearly identical. Therefore, the differences between these redox probes are due to different rates of the pseudo-unimolecular photoinduced charge transfer elementary step (which is directly controlled by the driving force) rather than chemical interactions with the QD. This observation contrasts with studies where the charge acceptor was bound to the quantum dot through a head group, and the identity of this head group controlled the rate of photoinduced charge transfer by controlling the binding equilibrium to the QD surface.[15]

The measured k_{PCT} values range from $1.5\text{-}5.1\times10^4$ $M^{-1}s^{-1}$ for the driving force series examined here. As a benchmark, the diffusion-controlled rate constant ($k_{diff,}$ the rate assuming every collision results in a charge transferred) is estimated by the Smoluchowski equation (**Eq. 3**), where R_{QD} and R_M are the radii of the QD and molecular charge acceptor, respectively, and D_{QD} and D_M are the diffusion coefficients.[42] Importantly, k_{diff} can be directly compared to the result from this work, as both describe bimolecular processes with the same units. Then, $k_{diff} \sim 10^{10}$ $M^{-1}s^{-1}$ is six orders of magnitude larger than k_{PCT} determined in this work. This implies that productive photoinduced charge transfer is a rare event in these experiments: for one million collisions, only one charge is effectively transferred to the charge acceptor. We believe the low k_{PCT} helps explain common observations that photocatalytic reactions suffer from extremely poor quantum yield.[18] We attribute the small k_{PCT} to the extremely weak electronic coupling between the inorganic QD core and M in solution. Either charges must tunnel through the ligand shell to reach M in solution or M must bury itself in the ligand shell to get better electronic overlap.[43] Importantly, this comparison highlights the practical utility of using CV to measure k_{PCT} in determining the potential of QD donors and molecular acceptors in a photocatalytic reaction scheme.

$$k_{diff} = \frac{4\pi N}{1000}\left(R_{QD} + R_M\right)\left(D_{QD} + D_M\right) = 4 \times 10^{10}\ (M\ \mathrm{s})^{-1} \qquad \text{Eq. 3}$$

Further, we can compare the observed rate constant (k_{obs}) to reported turn over frequencies (TOF) for homogeneous catalysts.[23] In this context, k_{obs} describes the moles of electrons transferred from QD to redox probe, per unit time per mole of the oxidized redox probe in the diffusion layer. Then, the TOF for the electron acceptors in this work ranges $0.5\text{-}1.5\times10^3$ hr^{-1}. In comparison, the well-known nitrogenase enzyme, which reduces N_2 to NH_3, was measured electrochemically to have an electron transfer TOF of 1.2×10^4 hr^{-1}.[44] Similarly, we can compare to photocatalytic systems. In an iridium photocatalytic system tuned for CO_2 reduction, the highest observed TOF was 22 hr^{-1}.[45] These benchmarks place photoinduced

electron transfer from QDs faster than reductive photocatalysis in a molecular system, but slower than an enzymatic reduction.

Net hole transfer: $CoCp_2$ and $CoCp_2COOH$

To expand the utility of this method, we considered two probes with lower E^0: cobaltocenium ($CoCp_2^+$) and cobaltocenium carboxylic acid ($CoCp_2COOH^+$). In illuminated CV experiments with these redox probes, the oxidative current decreases and the reductive current increases in a manner consistent with the E_rC_i' mechanism, indicating that there is effective photoinduced hole extraction from the QD (**Figure 5**). We are particularly excited by this result because it demonstrates that our method for measuring charge transfer can be generalized to hole transfer as well as electron transfer. This is in contrast with spectroscopic characterization, where electron and hole dynamics are difficult to isolate.[46]

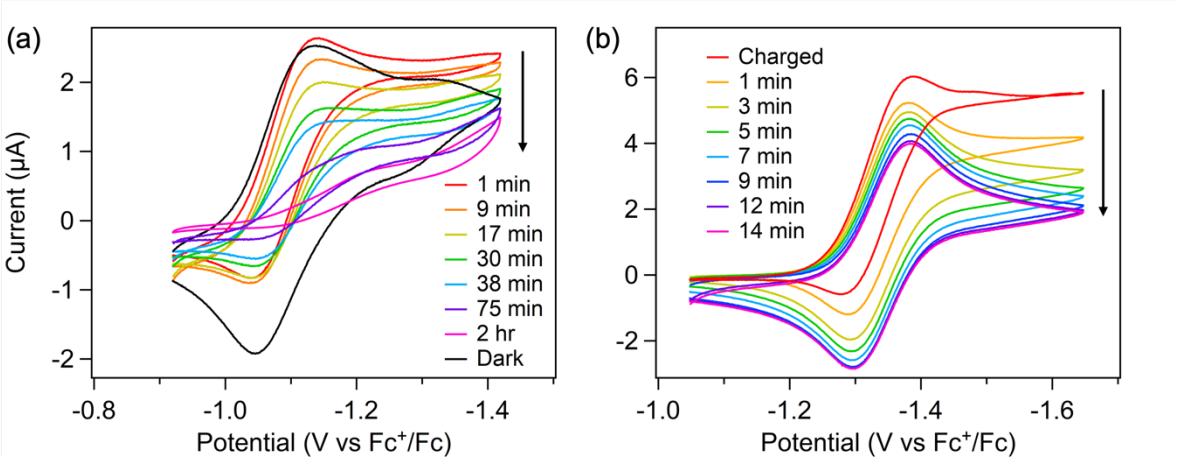

Figure 5. (a) CVs of $CoCp_2COOH^+$ without illumination (black) and showing photodecomposition over two hours of illumination (colors). (b) CVs of $CoCp_2^+$ monitored after illumination ends, demonstrating slow depletion of hole donor states. 0.1M [TBA][PF_6], benzonitrile, glassy carbon working, Pt counter, Ag wire pseudo reference electrodes, 10 mV/s.

Determination of the effective hole extraction rate is not viable with $CoCp_2COOH^+$. The dark CV shows two redox couples that are separated by 220 mV. When the CV scan rate is slowed from 250 mV/s to 5 mV/s, the relative current of the second wave to the first decreases. This indicates the species undergoing the second reduction is chemically formed from the product of the first reduction, or an ECE mechanism in the absence of illumination (**Figure S5**). Further, when the $CoCp_2COOH^+$ solution with QDs is illuminated, the CV first distorts as described above, but the current density decreases with extended illumination (minutes), indicating photodecomposition of $CoCp_2COOH^+$ (**Figure 5a**).

In the $CoCp_2^+$ solution, after illumination is begun the CV distorts over several minutes as described above, then the CVs stop changing. Similarly, when illumination is stopped, the CVs take several minutes before overlaying with the trace before illumination (**Figure 5b**). This indicates that, as in the case of electron transfer, the hole-donating species forms over several minutes under illumination before equilibration, and this hole-donating species is long-lived. We propose that this hole-donating species is

the hole trap that is populated during the n-type photodoping process and that is slowly depopulated when a conduction band electron recombines with localized holes. Trap mediated hole transfer to molecules has previously been demonstrated in similar QD systems.[11,40]

In the same manner as the electron acceptor series, the rate of photoinduced hole transfer to $CoCp_2$ was determined mathematically and through electrochemical modeling. Both methods require knowledge of the concentration of hole-donors, which we estimate is equal to the concentration of the QDs. The mathematical method gives k_{PCT} of 1.38×10^4 $M^{-1}s^{-1}$ and the modeling method gives 1.17×10^4 $M^{-1}s^{-1}$. Both results are slower than the slowest k_{PCT} in the electron transfer series. This is in good agreement with prior observations that in reductive photocatalysis, hole quenching rather than electron transfer to cocatalyst os rate limiting.[20,47] Uniquely, we are able to easily disentangle hole transfer dynamic from electron transfer by directly monitoring either oxidation or reduction of the molecular probe.

Conclusion

In this work, cyclic voltammetry has been used for the first time to quantify the rate of photoinduced charge transfer in solution. By carefully designing the photoelectrochemical cell and solvent/electrolyte combination, we were able to simultaneously irradiate and take CV data, generating dynamics that could be readily described by a two-reaction E_rC_i' mechanism. This technique is a powerful tool for screening photocatalytic systems by directly measuring the effective rate of charge extraction from a photosensitizer. By varying the redox potential of molecular charge acceptors, both net electron and hole transfer from photodoped colloidal quantum dots were observed. Using this technique, we were able to reproduce spectroscopic observation that the rate of photoinduced electron transfer from QDs increases monotonically with driving force. This method is especially compelling because it directly probes the changing oxidation state of the charge acceptor, in contrast with many other techniques that focus on the photophysics of the photosensitizer. The resulting rates of charge transfer, on the order of 10^4 $M^{-1}s^{-1}$, are distinct from the spectroscopically measured picosecond dynamics, and report on the rate of generation of charge separated states relevant to photocatalysis.

Supporting Information

Electronic supplementary information (ESI) available: Additional experimental (synthesis and electrochemistry) details, calculations, and supplementary data. See DOI: XXXXXX.

Corresponding Author

*cossairt@uw.edu

Funding Sources

National Science Foundation DMR-1719797

Acknowledgements

This material is based upon work supported by the National Science Foundation under award number DMR-1719797. This material is based in part upon work supported by the state of Washington through the University of Washington Clean Energy Institute. Part of this work was conducted at the Molecular Analysis Facility, a National Nanotechnology Coordinated Infrastructure site at the University of Washington which is supported in part by the National Science Foundation (grant NNCI-1542101), the University of Washington, the Molecular Engineering & Sciences Institute, and the Clean Energy Institute.

References

(1) Qiu, F.; Han, Z.; Peterson, J. J.; Odoi, M. Y.; Sowers, K. L.; Krauss, T. D. Photocatalytic Hydrogen Generation by CdSe/CdS Nanoparticles. *Nano Lett.* **2016**, *16* (9), 5347–5352. https://doi.org/10.1021/acs.nanolett.6b01087.

(2) Yu, W. W.; Qu, L.; Guo, W.; Peng, X. Experimental Determination of the Extinction Coefficient of CdTe, CdSe, and CdS Nanocrystals. *Chem. Mater.* **2003**, *15* (14), 2854–2860. https://doi.org/10.1021/cm034081k.

(3) Rabouw, F. T.; de Mello Donega, C. Excited-State Dynamics in Colloidal Semiconductor Nanocrystals. *Top. Curr. Chem.* **2016**, *374* (5), 58. https://doi.org/10.1007/s41061-016-0060-0.

(4) Graetzel, M.; Frank, A. J. Interfacial Electron-Transfer Reactions in Colloidal Semiconductor Dispersions. Kinetic Analysis. *J. Phys. Chem.* **1982**, *86* (15), 2964–2967. https://doi.org/10.1021/j100212a031.

(5) Wang, X.; Li, C. Interfacial Charge Transfer in Semiconductor-Molecular Photocatalyst Systems for Proton Reduction. *J. Photochem. Photobiol. C Photochem. Rev.* **2017**, *33*, 165–179. https://doi.org/10.1016/j.jphotochemrev.2017.10.003.

(6) Cho, E.; Kim, T.; Choi, S.; Jang, H.; Min, K.; Jang, E. Optical Characteristics of the Surface Defects in InP Colloidal Quantum Dots for Highly Efficient Light-Emitting Applications. *ACS Appl. Nano Mater.* **2018**, *1* (12), 7106–7114. https://doi.org/10.1021/acsanm.8b01947.

(7) Guyot-Sionnest, P.; Shim, M.; Matranga, C.; Hines, M. Intraband Relaxation in CdSe Quantum Dots. *Phys. Rev. B* **1999**, *60* (4), R2181–R2184. https://doi.org/10.1103/PhysRevB.60.R2181.

(8) Morris-Cohen, A. J.; Peterson, M. D.; Frederick, M. T.; Kamm, J. M.; Weiss, E. A. Evidence for a Through-Space Pathway for Electron Transfer from Quantum Dots to Carboxylate-Functionalized Viologens. *J. Phys. Chem. Lett.* **2012**, *3* (19), 2840–2844. https://doi.org/10.1021/jz301318m.

(9) Zhu, H.; Yang, Y.; Wu, K.; Lian, T. Charge Transfer Dynamics from Photoexcited Semiconductor Quantum Dots. *Annu. Rev. Phys. Chem.* **2016**, *67* (1), 259–281. https://doi.org/10.1146/annurev-physchem-040215-112128.

(10) Song, N.; Zhu, H.; Jin, S.; Zhan, W.; Lian, T. Poisson-Distributed Electron-Transfer Dynamics from Single Quantum Dots to C60 Molecules. *ACS Nano* **2011**, *5* (1), 613–621. https://doi.org/10.1021/nn1028828.

(11) Olshansky, J. H.; Balan, A. D.; Ding, T. X.; Fu, X.; Lee, Y. V.; Alivisatos, A. P. Temperature-Dependent Hole Transfer from Photoexcited Quantum Dots to Molecular Species: Evidence for Trap-Mediated Transfer. *ACS Nano* **2017**, *11* (8), 8346–8355. https://doi.org/10.1021/acsnano.7b03580.

(12) Buckley, J. J.; Couderc, E.; Greaney, M. J.; Munteanu, J.; Riche, C. T.; Bradforth, S. E.; Brutchey, R. L. Chalcogenol Ligand Toolbox for CdSe Nanocrystals and Their Influence on Exciton Relaxation Pathways. *ACS Nano* **2014**, *8* (3), 2512–2521. https://doi.org/10.1021/nn406109v.

(13) Morris-Cohen, A. J.; Frederick, M. T.; Cass, L. C.; Weiss, E. A. Simultaneous Determination of the Adsorption Constant and the Photoinduced Electron Transfer Rate for a Cds Quantum Dot–Viologen Complex. *J. Am. Chem. Soc.* **2011**, *133* (26), 10146–10154. https://doi.org/10.1021/ja2010237.

(14) Rawalekar, S.; Kaniyankandy, S.; Verma, S.; Ghosh, H. N. Ultrafast Charge Carrier Relaxation and Charge Transfer Dynamics of CdTe/CdS Core−Shell Quantum Dots as Studied by Femtosecond Transient Absorption Spectroscopy. *J. Phys. Chem. C* **2010**, *114* (3), 1460–1466. https://doi.org/10.1021/jp909118c.

(15) Morris-Cohen, A. J.; Aruda, K. O.; Rasmussen, A. M.; Canzi, G.; Seideman, T.; Kubiak, C. P.; Weiss, E. A. Controlling the Rate of Electron Transfer between a Quantum Dot and a Tri-Ruthenium Molecular Cluster by Tuning the Chemistry of the Interface. *Phys. Chem. Chem. Phys.* **2012**, *14* (40), 13794–13801. https://doi.org/10.1039/C2CP40827A.

(16) Knowles, K. E.; Peterson, M. D.; McPhail, M. R.; Weiss, E. A. Exciton Dissociation within Quantum Dot–Organic Complexes: Mechanisms, Use as a Probe of Interfacial Structure, and Applications. *J. Phys. Chem. C* **2013**, *117* (20), 10229–10243. https://doi.org/10.1021/jp400699h.

(17) Enright, M. J.; Gilbert-Bass, K.; Sarsito, H.; Cossairt, B. M. Photolytic C–O Bond Cleavage with Quantum Dots. *Chem. Mater.* **2019**, *31* (7), 2677–2682. https://doi.org/10.1021/acs.chemmater.9b00943.

(18) Zhang, Z.; Edme, K.; Lian, S.; Weiss, E. A. Enhancing the Rate of Quantum-Dot-Photocatalyzed Carbon–Carbon Coupling by Tuning the Composition of the Dot's Ligand Shell. *J. Am. Chem. Soc.* **2017**, *139* (12), 4246–4249. https://doi.org/10.1021/jacs.6b13220.

(19) Lu, H.; Zhu, X.; Miller, C.; San Martin, J.; Chen, X.; Miller, E. M.; Yan, Y.; Beard, M. C. Enhanced Photoredox Activity of CsPbBr3 Nanocrystals by Quantitative Colloidal Ligand Exchange. *J. Chem. Phys.* **2019**, *151* (20), 204305. https://doi.org/10.1063/1.5129261.

(20) Wu, K.; Chen, Z.; Lv, H.; Zhu, H.; Hill, C. L.; Lian, T. Hole Removal Rate Limits Photodriven H2 Generation Efficiency in CdS-Pt and CdSe/CdS-Pt Semiconductor Nanorod–Metal Tip Heterostructures. *J. Am. Chem. Soc.* **2014**, *136* (21), 7708–7716. https://doi.org/10.1021/ja5023893.

(21) Lian, S.; Weinberg, D. J.; Harris, R. D.; Kodaimati, M. S.; Weiss, E. A. Subpicosecond Photoinduced Hole Transfer from a CdS Quantum Dot to a Molecular Acceptor Bound Through an Exciton-Delocalizing Ligand. *ACS Nano* **2016**, *10* (6), 6372–6382. https://doi.org/10.1021/acsnano.6b02814.

(22) Woodward, J. R. Radical Pairs in Solution. *Prog. React. Kinet. Mech.* **2002**, *27* (3), 165–207. https://doi.org/10.3184/007967402103165388.

(23) Rountree, E. S.; McCarthy, B. D.; Eisenhart, T. T.; Dempsey, J. L. Evaluation of Homogeneous Electrocatalysts by Cyclic Voltammetry. *Inorg. Chem.* **2014**, *53* (19), 9983–10002. https://doi.org/10.1021/ic500658x.

(24) Costentin, C.; Fortage, J.; Collomb, M.-N. Electrophotocatalysis: Cyclic Voltammetry as an Analytical Tool. *J. Phys. Chem. Lett.* **2020**, *11* (15), 6097–6104. https://doi.org/10.1021/acs.jpclett.0c01662.

(25) Fukatsu, A.; Kondo, M.; Okamura, M.; Yoshida, M.; Masaoka, S. Electrochemical Response of Metal Complexes in Homogeneous Solution under Photoirradiation. *Sci. Rep.* **2014**, *4* (1), 5327. https://doi.org/10.1038/srep05327.

(26) Henckel, D. A.; Enright, M. J.; Panahpour Eslami, N.; Kroupa, D. M.; Gamelin, D. R.; Cossairt, B. M. Modeling Equilibrium Binding at Quantum Dot Surfaces Using Cyclic Voltammetry. *Nano Lett.* **2020**, *20* (4), 2620–2624. https://doi.org/10.1021/acs.nanolett.0c00162.

(27) Fox, M. A.; Akaba, R. Curve Crossing in the Cyclic Voltammetric Oxidation of 2-Phenylnorbornene. Evidence for an ECE Reaction Pathway. *J. Am. Chem. Soc.* **1983**, *105* (11), 3460–3463. https://doi.org/10.1021/ja00349a014.

(28) Araujo, J. J.; Brozek, C. K.; Kroupa, D. M.; Gamelin, D. R. Degenerately N-Doped Colloidal PbSe Quantum Dots: Band Assignments and Electrostatic Effects. *Nano Lett.* **2018**, *18* (6), 3893–3900. https://doi.org/10.1021/acs.nanolett.8b01235.

(29) Wu Lizhu; Huan Maoyong; Li Xubing; Zhou Shuai; Zhang Liping; Tong Zhenhe. Method for Photocatalytic Halogenation Conversion of Halogenated Hydrocarbon Using Quantum Dot/Rod Photocatalyst. CN109438156A.

(30) De Roo, J.; Yazdani, N.; Drijvers, E.; Lauria, A.; Maes, J.; Owen, J. S.; Van Driessche, I.; Niederberger, M.; Wood, V.; Martins, J. C.; Infante, I.; Hens, Z. Probing Solvent–Ligand Interactions in Colloidal Nanocrystals by the NMR Line Broadening. *Chem. Mater.* **2018**, *30* (15), 5485–5492. https://doi.org/10.1021/acs.chemmater.8b02523.

(31) Monahan, M.; Homer, M.; Zhang, S.; Zheng, R.; Chen, C.-L.; De Yoreo, J.; Cossairt, B. M. Impact of Nanoparticle Size and Surface Chemistry on Peptoid Self-Assembly. *ACS Nano* **2022**. https://doi.org/10.1021/acsnano.2c01203.

(32) Geiger, W. E.; Barrière, F. Organometallic Electrochemistry Based on Electrolytes Containing Weakly-Coordinating Fluoroarylborate Anions. *Acc. Chem. Res.* **2010**, *43* (7), 1030–1039. https://doi.org/10.1021/ar1000023.

(33) Swarts, P. J.; Conradie, J. Solvent and Substituent Effect on Electrochemistry of Ferrocenylcarboxylic Acids. *J. Electroanal. Chem.* **2020**, *866*, 114164. https://doi.org/10.1016/j.jelechem.2020.114164.

(34) Shulenberger, K. E.; Keller, H. R.; Pellows, L. M.; Brown, N. L.; Dukovic, G. Photocharging of Colloidal CdS Nanocrystals. *J. Phys. Chem. C* **2021**, *125* (41), 22650–22659. https://doi.org/10.1021/acs.jpcc.1c06491.

(35) Zeng, Y.; Kelley, D. F. Excited Hole Photochemistry of CdSe/CdS Quantum Dots. *J. Phys. Chem. C* **2016**, *120* (31), 17853–17862. https://doi.org/10.1021/acs.jpcc.6b06282.

(36) Tsui, E. Y.; Carroll, G. M.; Miller, B.; Marchioro, A.; Gamelin, D. R. Extremely Slow Spontaneous Electron Trapping in Photodoped N-Type CdSe Nanocrystals. *Chem. Mater.* **2017**, *29* (8), 3754–3762. https://doi.org/10.1021/acs.chemmater.7b00839.

(37) Deblock, L.; Pokratath, R.; Buysser, K. D.; Roo, J. D. Mapping out the Aqueous Surface Chemistry of Metal Oxide Nanocrystals; Carboxylate, Phosphonate and Catecholate Ligands. **2021**. https://doi.org/10.26434/chemrxiv-2021-zjnrt.

(38) Kanicky, J. R.; Shah, D. O. Effect of Degree, Type, and Position of Unsaturation on the PKa of Long-Chain Fatty Acids. *J. Colloid Interface Sci.* **2002**, *256* (1), 201–207. https://doi.org/10.1006/jcis.2001.8009.

(39) Wang, L.-W.; Califano, M.; Zunger, A.; Franceschetti, A. Pseudopotential Theory of Auger Processes in CdSe Quantum Dots. *Phys. Rev. Lett.* **2003**, *91* (5), 056404. https://doi.org/10.1103/PhysRevLett.91.056404.

(40) Olshansky, J. H.; Ding, T. X.; Lee, Y. V.; Leone, S. R.; Alivisatos, A. P. Hole Transfer from Photoexcited Quantum Dots: The Relationship between Driving Force and Rate. *J. Am. Chem. Soc.* **2015**, *137* (49), 15567–15575. https://doi.org/10.1021/jacs.5b10856.

(41) Nagelj, N.; Brumberg, A.; Peifer, S.; Schaller, R. D.; Olshansky, J. H. Compositionally Tuning Electron Transfer from Photoexcited Core/Shell Quantum Dots via Cation Exchange. *J. Phys. Chem. Lett.* **2022**, 3209–3216. https://doi.org/10.1021/acs.jpclett.2c00333.

(42) Joseph Lakowicz. *Principles of Fluorescence Spectroscopy*, 3rd ed.; Springer: Baltimore, 2006.

(43) Huang, Y.; Cohen, T. A.; Sperry, B. M.; Larson, H.; Nguyen, H. A.; Homer, M. K.; Dou, F. Y.; Jacoby, L. M.; Cossairt, B. M.; Gamelin, D. R.; Luscombe, C. K. Organic Building Blocks at Inorganic Nanomaterial Interfaces. *Mater. Horiz.* **2022**, *9* (1), 61–87. https://doi.org/10.1039/D1MH01294K.

(44) Gu, W.; Milton, R. D. Natural and Engineered Electron Transfer of Nitrogenase. *Chemistry* **2020**, *2* (2), 322–346. https://doi.org/10.3390/chemistry2020021.

(45) Genoni, A.; Chirdon, D. N.; Boniolo, M.; Sartorel, A.; Bernhard, S.; Bonchio, M. Tuning Iridium Photocatalysts and Light Irradiation for Enhanced CO2 Reduction. *ACS Catal.* **2017**, *7* (1), 154–160. https://doi.org/10.1021/acscatal.6b03227.

(46) Morgan, D. P.; Kelley, D. F. What Does the Transient Absorption Spectrum of CdSe Quantum Dots Measure? *J. Phys. Chem. C* **2020**, *124* (15), 8448–8455. https://doi.org/10.1021/acs.jpcc.0c02566.

(47) Berr, M. J.; Wagner, P.; Fischbach, S.; Vaneski, A.; Schneider, J.; Susha, A. S.; Rogach, A. L.; Jäckel, F.; Feldmann, J. Hole Scavenger Redox Potentials Determine Quantum Efficiency and Stability of Pt-Decorated CdS Nanorods for Photocatalytic Hydrogen Generation. *Appl. Phys. Lett.* **2012**, *100* (22), 223903. https://doi.org/10.1063/1.4723575.